Available online at www.sciencedirect.com

ScienceDirect

Computational Materials Science 00 (2016) 1–8

Computational Materials Science

# Selecting reliable interatomic potentials for classical molecular dynamics simulations of glasses: the case of amorphous $SiO_2$

N.D. Afify[a,b,*], G. Mountjoy[b], R. Haworth[c]

[a]*Egypt Nanotechnology Research Center, El-Sheikh Zayed City, Giza, Egypt*
[b]*School of Physical Sciences, University of Kent, Canterbury CT2 7NH, United Kingdom*
[c]*Akeley Wood School, Bycell Road, Akeley Wood, Buckingham, MK18 5AE, UK*

**Abstract**

This paper presents an approach to judge the quality of classical interatomic potentials used in molecular dynamics simulations of glasses. The static structure and dynamical properties of amorphous $SiO_2$ were simulated by classical molecular dynamics using a series of well known interatomic potentials. Theoretical X-ray and neutron structure factors and effective neutron-weighted vibrational density of states of amorphous $SiO_2$ were computed from the obtained atomistic configurations and quantitatively compared to experimental results. The interatomic potential which best reproduced the experimental X-ray and neutron scattering data severely failed to reproduce the experimental vibrational density of states of amorphous $SiO_2$. It is found that only the potential developed by van Beest, Kramer, and van Santen (BKS) was able to adequately reproduce both static structure and dynamical properties of amorphous $SiO_2$. Thus, the fact that an interatomic potential is able to properly reproduce static structures of amorphous systems should not be considered as a basis to use this potential to simulate other properties of these systems.

*Keywords:* Classical interatomic potential, Molecular dynamics, Amorphous $SiO_2$, Vibrational density of states, X-ray scattering, Neutron scattering

## 1. Introduction

Classical molecular dynamics simulation is a very powerful technique able to give detailed information on static structures and dynamical properties of amorphous materials. Since an interatomic potential is the main ingredient of any classical molecular dynamics simulation study, the accuracy of the obtained results are strongly dependent on the used potential. The absence of any unique approach to judge the quality of an interatomic potential by classical molecular dynamics users can lead to unreliable results and conclusions. Thus, the way the quality of an interatomic potential is judged for a particular molecular dynamics study is an important issue that needs to be properly addressed.

The majority of molecular dynamics users do not usually develop their own classical interatomic potentials. In this case, different classical interatomic potentials are usually collected from the literature and a decision on the most accurate potential has to be made. The most common approach to make this decision is to use the available interatomic potentials to predict structures and physical properties of crystals related to the amorphous system under study, and compare the resulting predictions to available experimental results. In this paper we will demonstrate that such approach may lead to incorrect choice of which interatomic potential is the best. The previous approach does not guarantee that the high quality of the chosen interatomic potential will be maintained in the simulation of

*Corresponding author
*Email address:* nasser.afify@egnc.gov.eg (N.D. Afify)

amorphous samples. This will depend on the transferability of interatomic potential from crystals to their amorphous counterparts. It will also depend on whether we are interested only in simulating static structures of amorphous systems or also interested in simulating other properties.

When using molecular dynamics simulation to study structures of amorphous materials the quality of the used interatomic potentials should be further validated by comparing experimental scattering spectra to the scattering spectra computed from the obtained molecular dynamics atomistic models. In this case it is important to resort to experimental scattering data from different sources such as X-rays and neutrons. It is also important to resort to scattering spectra in reciprocal space since Fourier transformed spectra are usually manipulated to account for the limited data range. The comparison between experimental and molecular dynamics derived scattering data is usually done at qualitative level. However, it is more accurate to quantitatively evaluate the degree of agreement between the experimental and calculated spectra. As will be demonstrated in this paper, even if all the above precautions are accounted for there still no guarantee that the selected interatomic potential will behave adequately when this potential is used in the simulation of properties other than static structures.

## 2. Computational details

In the current study, we carried out classical molecular dynamics simulations on amorphous $SiO_2$ using several interatomic pair potentials. Our choice of the amorphous $SiO_2$ system is justified by the fact that amorphous $SiO_2$ is the most experimentally and computationally studied amorphous system. The methodologies and approaches used in this study are, however, applicable to any other amorphous system. We considered the following well-known interatomic pair potentials of amorphous $SiO_2$: (i) TTAM: developed by Tsuneyuki et al. [1], (ii) BKS: developed by Van Beest et al. [2], (iii) T: developed by Teter [3], (iv) FB: developed by Flikkema et al. [4], (v) DC: developed by Cormack et al. [5], and (vi) PMMCS, developed by Pedone et al. [6]. Acronyms of the potentials names stand for the initials of the authors who have developed or further refined these potentials. The first five are Buckingham potential type while the last one is Morse potential type [7]. All the considered interatomic potentials use partial ionic charges of +2.4 and -1.2 for the silicon and oxygen atoms respectively.

We first used the general utility lattice program (GULP) [7] to test the ability of the different interatomic pair potentials to predict the lattice constants and some physical properties of the alpha-quartz form of crystalline $SiO_2$. The GULP free energy calculations were carried out at ambient temperature and pressure. For all the tested interatomic potentials, GULP calculations were made up to a cut-off of 15 Å for the Si-O, O-O, and Si-Si atomic pairs. Classical molecular dynamics simulations of amorphous $SiO_2$ were carried out using the DLPOLY 2.18 code [8]. This code was modified by the current authors to simulate the melt-quenching process, required to simulate amorphous $SiO_2$ structures. For each interatomic potential the simulated sample contained 3000 atoms randomly placed in a cubic box with a room temperature density of 2.2 g/cm$^3$. The periodic boundary conditions applied in all directions. The long-range Coulombic interactions were evaluated by the Ewald method, using a real space cut-off of 12.0 Å, and an Ewald precision factor of $10^{-5}$ [8]. The short-range interactions cut-off was set to 7.6 Å. The classical Newton's equation of motion were integrated using the Verlet Leapfrog algorithm [8]. Our classical molecular dynamics simulations used a time step of 1 fs.

Each molecular dynamics simulation comprised six simulation stages. In the first three stages, the system was melted and equilibrated at the temperatures 6000 K, 3500 K, and 2200 K, each for a time duration of 80 ps. The simulated system density was adjusted at the different temperatures to account for thermal expansion. In the fourth stage, the system was continuously quenched from 2200 K to 300 K in a time duration of 95 ps, with a nominal quenching rate of $1.0\times10^{13}$ K/s. During the optimization of our molecular dynamics simulation framework we tested the following three quenching rates: $5.0\times10^{11}$ K/s, $1.0\times10^{12}$ K/s, and $1.0\times10^{13}$ K/s. For these three quenching rates the system was quenched down from 2200 K to 300 K in a time duration of 95 ps, 950 ps, and 1900 ps respectively. In Figure 1 of the Supporting Materials we report the neutron and X-ray weighted total static structure factors produced by the BKS [2] interatomic pair potential using these different quenching rates. From the great similarity between the reported structure factors we concluded that as far as high computational quenching rates are concerned, our choice of the quenching rate $1.0\times10^{13}$ K/s is justified.

In the fifth stage, the system was equilibrated at the room temperature for a time duration of 80 ps. Finally, structural snapshots were collected in the sixth stage for a time duration of 80 ps, with a time interval of 0.05 ps, leading therefore to 1600 atomistic configuration in the final trajectory. The NVT ensemble was used during all the simulation

stages except for the fifth simulation stage, where the NVT simulation was followed by another NPT simulation for an additional time duration of 80 ps.. This procedure was found to produce amorphous $SiO_2$ samples with accurate bond angles distributions [9]. For each interatomic potential, three independent molecular dynamics simulations starting from different random configurations, were performed to assess the statistical accuracy of molecular dynamics results.

In the following we demonstrate that our procedure of sampling molecular dynamics trajectories at the room temperature is adequate. Using the BKS [2] interatomic pair potential we rerun the sixth simulation stage for time durations of 400 ps and 2000 ps, with time intervals of 0.025 ps and 0.125 ps respectively, leading therefore to 16000 atomistic configuration in each trajectory. In Figure 2 of the Supporting Materials we report the resulting neutron and X-ray weighted pair distribution functions $g(R)$ using these two additional sampling procedures compared to the neutron and X-ray weighted pair distribution functions obtained using the sampling procedure mentioned in the previous paragraph. From the excellent agreement between the resulting pair distribution functions we concluded that our choice of the sampling procedure at the room temperature is adequate.

The X-ray and neutron static structure factors $S(Q)$ were calculated using the ISAACS code [25]. To calculate the static structure factor $S(Q)$ from the obtained molecular dynamics atomistic configurations we first calculated the real space partial pair distribution functions $T_{\alpha\beta}(r)$ using Equation 1. In this equation, $\alpha$ and $\beta$ are the element types. The $Q$-weighted structure factors $Q(S(Q)-1)$ were then calculated using Equation 2, where $Q$ is the scattering vector, $w_{\alpha\beta}$ are X-ray or neutron weighting factors, $c_\beta$ is the fractional concentration of the element $\beta$, and $\rho_0$ is average atomic number density [10]. These static structure factor $S(Q)$ calculations we repeated on 1600 atomistic configurations and final averages were obtained.

$$T_{\alpha\beta}(r) = \frac{1}{r}\left(\frac{1}{N_\alpha}\sum_{i=1}^{N_\alpha}\sum_{j=1}^{N_\beta}\delta\left(r - R_{ij}\right)\right) \tag{1}$$

$$Q\left(S\left(Q\right)-1\right) = \sum_{\alpha\beta} w_{\alpha\beta}(Q)\int\left(T_{\alpha\beta}(r)\Big/c_\beta - 4\pi r\rho_0\right)\sin(Qr)\,dr \tag{2}$$

For each interatomic potential the neutron-weighted vibrational density of states $VDOS$ was calculated from the obtained molecular dynamics configurations as follows. As shown in equation 3, in a multicomponent system, the true partial vibrational density of states of an atomic species $\alpha$ is the time-domain Fourier transform of the velocity autocorrelation function $C^{\alpha}_{vv}$ of this species. Silicon and oxygen true partial vibrational density of states ($g_{Si}(\omega)$ and $g_O(\omega)$) were calculated according to equation 3 using the nMOLDYn 2.5 code [11]. The effective neutron-weighted total vibrational density of states $VDOS(\omega)$ was then calculated from the partials $g_{Si}(\omega)$ and $g_O(\omega)$ using equation 4. In this equation, $c_\alpha$, $\sigma_\alpha$, $m_\alpha$, and $W_\alpha$ are the atomic fractional concentration, neutron scattering cross-section, atomic mass, and Debye-Waller factor of the element $\alpha$. The normalization factor $N$ was chosen such that $\int g(\omega)\,d\omega = 1$. The thermal term $\exp(-2W_\alpha)$ was approximated by unity for both silicon and oxygen atoms [12, 13] since in the case of amorphous $SiO_2$ at room temperature the thermal disorder can be neglected when compared to the static disorder.

$$g_\alpha(\omega) = \int_0^\infty \exp(-i\omega t)\,C^{\alpha}_{vv}(t)\,dt \tag{3}$$

$$VDOS = \frac{1}{N}\sum_{\alpha}\left(\frac{c_\alpha\sigma_\alpha}{m_\alpha}\right)g_\alpha(\omega)\exp(-2W_\alpha) \tag{4}$$

## 3. Results and discussion

In this section we present and discuss our results on how to select the most reliable interatomic potential for classical molecular dynamics simulations of amorphous $SiO_2$. We start by reporting the ability of the selected interatomic pair potentials to correctly reproduce the experimentally observed lattice constants and some physical properties of crystalline $SiO_2$ according to the obtained GULP results. In Table 1 we report a comparison between experimental

Table 1. Experimental [14, 15, 16] and GULP predicted lattice constants, elastic constants, and bulk and shear moduli for the alpha-quartz form of crystalline $SiO_2$ using the TTAM [1], BKS [2], T [3], FB [4], DC [5], and PMMCS [6] interatomic pair potentials.

| Interatomic potential | lattice parameters [Å] | | elastic constants [GPa] | | | | | | | bulk modulus [GPa] | shear modulus [GPa] |
|---|---|---|---|---|---|---|---|---|---|---|---|
| | a | c | $C_{11}$ | $C_{12}$ | $C_{13}$ | $C_{14}$ | $C_{33}$ | $C_{44}$ | $C_{66}$ | | |
| Experimental | 4.9147 | 5.4066 | 86.7 | 7.0 | 11.9 | -17.9 | 107.2 | 57.9 | 39.8 | 36.4 | 31.1 |
| TTAM | 5.0065 | 5.5478 | 67.1 | 10.8 | 13.0 | -12.6 | 94.0 | 38.4 | 28.1 | 32.7 | 28.9 |
| BKS | 4.9214 | 5.4335 | 89.5 | 10.2 | 16.9 | -16.9 | 111.9 | 50.6 | 39.7 | 41.4 | 38.9 |
| T | 4.9353 | 5.4452 | 91.1 | 2.6 | 9.3 | -19.1 | 92.3 | 47.7 | 44.3 | 35.1 | 38.4 |
| FB | 5.3632 | 5.8887 | 101.3 | -9.8 | 5.1 | -10.0 | 75.9 | 39.8 | 55.5 | 30.9 | 42.6 |
| DC | 5.0310 | 5.5477 | 103.8 | -6.4 | 4.3 | -19.3 | 85.7 | 47.6 | 55.1 | 33.1 | 43.4 |
| PMMCS | 4.9220 | 5.4309 | 87.2 | 8.8 | 11.8 | -17.8 | 106.6 | 49.7 | 39.2 | 38.0 | 37.9 |

[14, 15, 16] and GULP predicted lattice constants, elastic constants, and bulk and shear moduli for the alpha-quartz form of crystalline $SiO_2$ using the TTAM [1], BKS [2], T [3], FB [4], DC [5], and PMMCS [6] interatomic potentials.

From this table it can be seen that the theoretical GULP predictions based on the PMMCS interatomic potentials are the closest to the experimental results. On contrary, the poorest agreement between experimental and calculated results occur in the case of the FB interatomic potential. It can be also seen that GULP predictions are very similar in the cases of the PMMCS and BKS interatomic potentials. Based on these GULP evaluations a significant part of molecular dynamics users would select the PMMCS or BKS interatomic potentials to simulate the static structure and dynamical properties of amorphous $SiO_2$. It will be shown however that such conclusion is not entirely transferable to the simulation of amorphous $SiO_2$.

Now we discuss the ability of classical molecular dynamics simulations based on the selected interatomic pair potentials to reproduce the static structure and dynamical properties of amorphous $SiO_2$. The static structure is experimentally represented by the total X-ray and neutron static structure factors $S(Q)$. The dynamical properties are experimentally represented by the effective neutron-weighted vibrational density of states $VDOS$. Figure 1 compares the experimental (black solid lines) and classical molecular dynamics derived (red dotted lines) neutron (Figure 1(a)) and X-ray (Figure 1(b)) total static structure factors $Q(S(Q)-1)$ using the TTAM [1], BKS [2], T [3], FB [4], DC [5], and PMMCS [6] interatomic potentials. The neutron scattering data were taken from Grimley et al. [17] and X-ray data were collected on the BM08 GILDA Beamline of the European Synchrotron Radiation Facility (ESRF). In these figures the total X-ray and neutron structure factors $S(Q)$ are weighted by the scattering vector $Q$ to emphasize short range order information at large scattering vector values.

From Figures 1(a) and 1(b) we can see that the calculated structure factors based on the PMMCS interatomic potential show the best agreement with the experimental data. On contrary, the calculated structure factors reproduced by the FB potential possess the poorest agreement with experimental data. In fact, this potential produces a structure with overestimated interatomic distances as evidenced by the significant shift of $Q(S(Q)-1)$ features to lower $Q$ values. This feature is also present in the previous GULP calculations on crystalline $SiO_2$. Based on both Figure 1 and the previous GULP results it may be concluded that the PMMCS potential would be the best candidate interatomic potential for classical molecular dynamics simulation of amorphous $SiO_2$. In fact, Afify et al. have claimed the superiority of this potential in modelling the static structure of $Eu^{3+}$-doped $SiO_2$ glasses [9]. In the following paragraphs we will show that this approach can not be considered as a global interatomic potential choice criteria. We will show that this approach can be correct only if the static structure of amorphous $SiO_2$ is the only property required from classical molecular dynamics simulations of amorphous $SiO_2$.

In Figure 2 we compare the experimental (black solid lines) and classical molecular dynamics derived (red dotted lines) effective neutron-weighted vibrational density of states $VDOS(\omega)$ of amorphous $SiO_2$ for the different interatomic pair potentials. The experimental $VDOS(\omega)$ was derived from the time-of-flight inelastic neutron scattering data collected by the current authors using the MARI instrument installed at the ISIS facility [18]. Surprisingly, Figure 2 demonstrates that the PMMCS interatomic potential has a very poor ability to reproduce the experimental vibrational density of states of amorphous $SiO_2$. This important result shows that the fact that an interatomic potential has a great capability to reproduce the static structure of an amorphous system does not mean that the same potential can be trusted in simulating other properties such as dynamical properties. It can be immediately seen from Figure

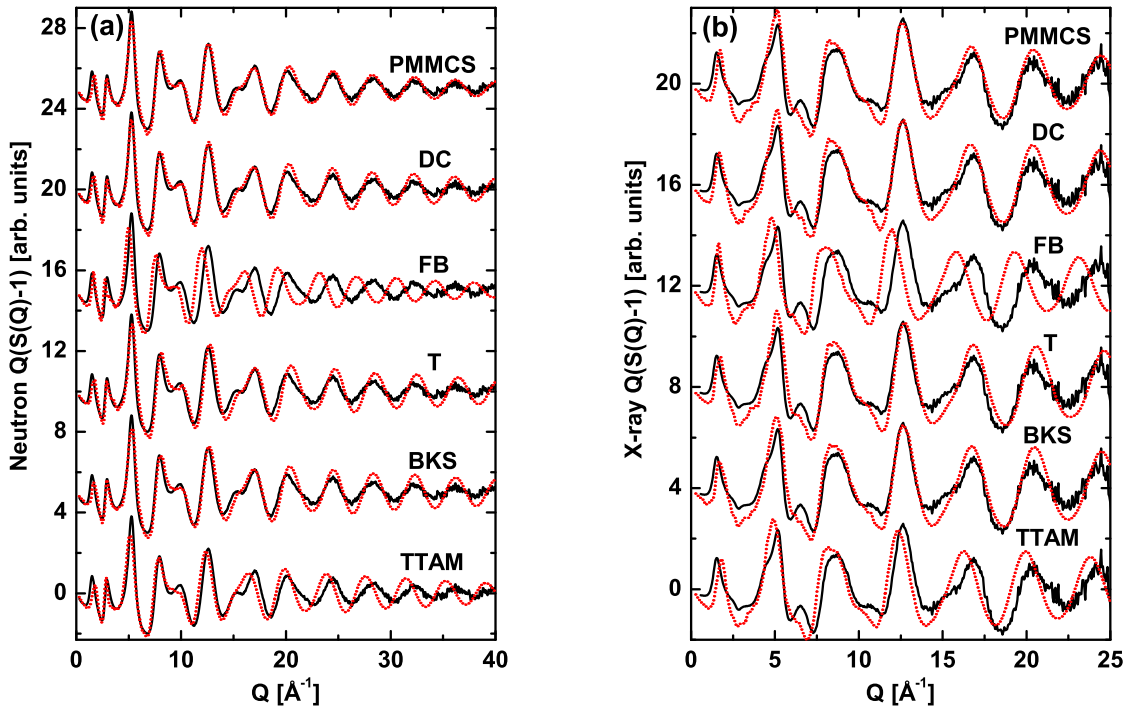


(a) (b)

Figure 1. Comparison between the experimental (black solid lines) and classical molecular dynamics derived (red dotted lines) total static structure factors $Q(S(Q)-1)$ based on the TTAM [1], BKS [2], T [3], FB [4], DC [5], and PMMCS [6] interatomic pair potentials: (a) neutron scattering data, and (b) X-ray scattering data. The total X-ray and neutron structure factors $S(Q)$ are weighted by $Q$ to emphasize short range order information at large scattering vector values.

2 that only the BKS interatomic potential is able to predict the correct positions and widths of the double-peak in the region 30-40 $THz$ of the vibrational spectrum of amorphous $SiO_2$. This doublet originates from the symmetric and asymmetric stretches of $SiO_4$ units in amorphous $SiO_2$ [19, 18]. We note from Figure 2 that none of the used interatomic pair potentials was able to reproduce the $VDOS(\omega)$ peaks centred around 25 $THz$ and 35 $THz$. Modelling of these peaks requires the inclusion of many-body terms in these pair potentials.

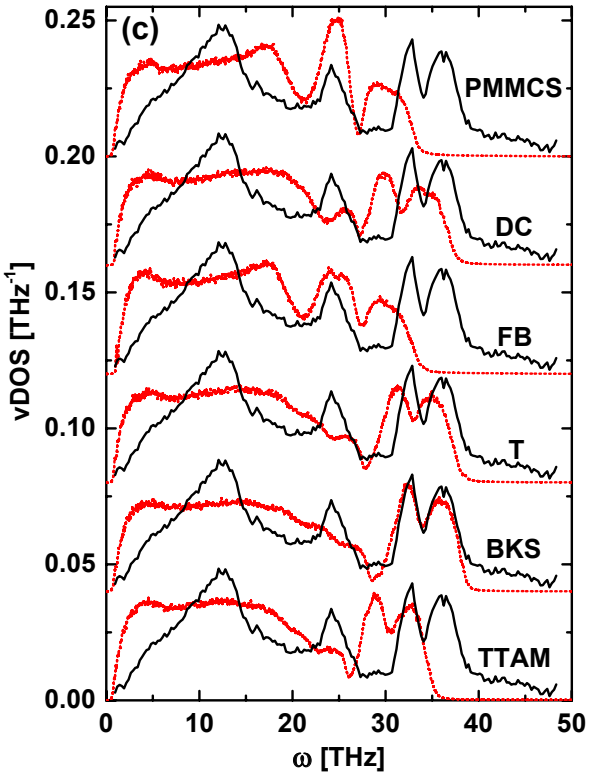


Figure 2. Comparison between the experimental (black solid lines) and classical molecular dynamics derived (red dotted lines) neutron-weighted vibrational density of states $VDOS(\omega)$ of amorphous $SiO_2$ based on the TTAM [1], BKS [2], T [3], FB [4], DC [5], and PMMCS [6] interatomic pair potentials.

In the following we quantitatively evaluate the ability of classical molecular dynamics simulations based on the TTAM [1], BKS [2], T [3], FB [4], DC [5], and PMMCS [6] interatomic pair potentials to reproduce both static structure and dynamical properties of amorphous $SiO_2$. In Table 2 we report the experimental and classical molecular dynamics simulations derived number density $\rho$ , Si-O average interatomic distance ($\langle r_{Si-O} \rangle$), Si-O Debye-waller factor ($\sigma^2_{Si-O}$), and Si-O-Si average bond angle ($\langle \text{Si} - \hat{\text{O}} - \text{Si} \rangle$). The quantitative agreement between the experimental and classical molecular dynamics derived results are given for the different potentials by the $R$-factors $R_{Static-ND}$, $R_{Static-XRD}$, and $R_{Dynamic-VDOS}$, which represent the residual factors for neutron scattering, X-ray scattering, and vibrational density of states spectra respectively. The reported $R$-factors were calculated using Equation 5, where $f_{\exp}(x)$, $f_{MD}(x)$, and $N$ are the experimental and classical molecular dynamics simulations derived spectra, and the number of experimental data points respectively. To simplify the comparison between the different interatomic potentials the values of the different $R$-factors were normalized by the largest $R$ value. Thus, an interatomic potential with poorest agreement with experimental results would result in $R$-factor of one. In Table 2 the quality rank of the different interatomic potentials are reported in square brackets.

$$\mathrm{R} = \frac{1}{\mathrm{N}} \sum_{i}^{N} \left( f_{\exp}(x) - f_{MD}(x) \right)^2 \tag{5}$$

Table 2. Comparison between the experimental and classical molecular dynamics simulations derived number density $\rho$, Si-O average interatomic distance ($\langle r_{Si-O} \rangle$), Si-O Debye-waller factor ($\sigma^2_{Si-O}$), and Si-O-Si average bond angle ($\langle \text{Si} - \hat{\text{O}} - \text{Si} \rangle$). $R_{Static-ND}$, $R_{Static-XRD}$, and $R_{Dynamic-VDOS}$ represent the residual $R$-factors for neutron scattering, X-ray scattering, and vibrational density of states spectra respectively. The quality rank of each interatomic potentials is reported in a square brackets.

| Interatomic potential | $\rho$ [$atoms/\text{Å}^3$] | $\langle r_{Si-O} \rangle$ [Å] | $\sigma^2_{Si-O}$ [$\text{Å}^2$] | $\langle \text{Si} - \hat{\text{O}} - \text{Si} \rangle$ [$^o$] | $R_{Static-ND}$ | $R_{Static-XRD}$ | $R_{Dynamic-vDOS}$ |
|---|---|---|---|---|---|---|---|
| Experimental | 0.06615 | 1.608(4) | 0.002(11) | 147.9 | | | |
| TTAM | 0.06991 | 1.6520(5) | 0.00132(5) | 147.8(2) | 0.38 [5] | 0.37 [5] | 0.84 [4] |
| BKS | 0.07047 | 1.6084(2) | 0.00111(3) | 147.4(2) | 0.17 [3] | 0.16 [3] | 0.29 [1] |
| T | 0.07048 | 1.5981(1) | 0.00114(2) | 150.0(1) | 0.20 [4] | 0.18 [4] | 0.44 [2] |
| FB | 0.06241 | 1.7035(3) | 0.00183(2) | 148.6(3) | 1.00 [6] | 1.00 [6] | 0.96 [5] |
| DC | 0.06867 | 1.6129(2) | 0.00120(5) | 151.1(1) | 0.11 [2] | 0.15 [2] | 0.59 [3] |
| PMMCS | 0.07035 | 1.6121(1) | 0.00180(3) | 149.5(3) | 0.09 [1] | 0.13 [1] | 1.00 [6] |

From the quality indexes reported in Table 2 it can be seen that from static structure point of view the PMMCS interatomic potential has the highest quality. On contrary, the FB pair interatomic potential has the lowest ability to reproduce the static structure of amorphous $SiO_2$. Regarding dynamical properties of amorphous $SiO_2$, Table 2 shows that the BKS interatomic potential has the highest quality in reproducing the experimental vibrational density of states of amorphous $SiO_2$. However, the PMMCS potential has the lowest ability to reproduce such dynamical properties. Therefore, if we are interested in simulating both static structure and dynamical properties of amorphous $SiO_2$, then the BKS potential would be our best choice since this potential is able to reasonably reproduce both static and dynamical properties of this amorphous system.

In the following we further verify the superiority of the BKS [2] potential in reproducing other properties of amorphous $SiO_2$. In Table 3 we report the self-diffusion coefficient $D$, heat capacity at constant pressure $c_p$, and isothermal compressibility $\beta$ of amorphous $SiO_2$ as derived from our molecular dynamics simulations using the TTAM [1], BKS [2], T [3], FB [4], DC [5], and PMMCS [6] interatomic pair potentials. The self-diffusion coefficients of silicon and oxygen and their ratio are reported at both room temperature and 1000 K. Experimental results of the heat capacity at constant pressure [21] and isothermal compressibility [20] are reported in the same table for comparison.

The self-diffusion coefficients of silicon and oxygen were calculated from the slope of the time dependence of mean square displacements (MSD) [23] of silicon and oxygen atoms. The molecular dynamics trajectories used in these calculations were 800 ps long. The time dependence of mean square displacements of silicon and oxygen at 1000 K are plotted in Figure 3 of the Supporting Materials. The heat capacity at constant pressure $c_p$ was calculated from fluctuations of the total energy [22] during the NPT simulation (i.e. the second half of the fifth simulation stage). To calculate the isothermal compressibility $\beta$ we carried out several room temperature NPT simulations at different pressures for each pair potential. The isothermal compressibility was then calculated from the slop of pressure-volume data [24]. The obtained pressure-volume results are reported in Figure 4 of the Supporting Materials.

Table 3. Self-diffusion coefficients $D$, heat capacity at constant pressure $c_p$, and isothermal compressibility $\beta$ of amorphous $SiO_2$ derived from molecular dynamics simulations using the TTAM [1], BKS [2], T [3], FB [4], DC [5], and PMMCS [6] interatomic pair potentials. The self-diffusion coefficients of silicon and oxygen and their ratio are reported at both room temperature and 1000 K. Experimental results of the heat capacity at constant pressure [21] and isothermal compressibility [20] are reported for comparison.

| Interatomic potential | $D$ at 300 K [$1.0 \times 10^{-15}$ $m^2/s$] | | | $D$ at 1000 K [$1.0 \times 10^{-13}$ $m^2/s$] | | | $c_p$ [J/Kg.K] | $\beta$ [$1.0 \times 10^{-11}$ $Pa^{-1}$] |
|---|---|---|---|---|---|---|---|---|
| | Si | O | $D$(O)/$D$(Si) | Si | O | $D$(O)/$D$(Si) | | |
| Experimental | | | 1.75 | | | 1.75 | 703.0 [21] | 1.20 [20] |
| TTAM | 27.45 | 40.60 | 1.48 | 1.32 | 1.52 | 1.15 | 564.1 | 2.55 |
| BKS | 0.43 | 0.70 | 1.63 | 0.84 | 1.24 | 1.48 | 620.9 | 2.64 |
| T | -0.41 | -0.70 | 1.71 | 0.39 | 0.50 | 1.31 | -1048.7 | 4.25 |
| FB | -2.72 | -3.68 | 1.35 | 1.22 | 1.53 | 1.25 | -458.9 | 4.58 |
| DC | 0.06 | 0.08 | 1.43 | 0.02 | 0.02 | 1.00 | 1003.3 | 4.84 |
| PMMCS | 6.31 | 10.95 | 1.74 | 1.25 | 1.44 | 1.15 | -107.9 | 3.66 |

First we comment on the self-diffusion results. Unfortunately, we could not find any experimental values for the silicon and oxygen self-diffusion coefficients measured at 300 K and 1000 K. From Table 3 we note that some interatomic potentials produced negative room-temperature self-diffusion coefficients of silicon and oxygen, which is not

physical in the case of amorphous $SiO_2$. This behaviour can be attributed to either an incapability of these interatomic potentials or to the fact that the determination of self-diffusion coefficients at the room temperature requires running simulations for an extremely long time.

To judge the capabilities of the different pair potentials in reproducing the self-diffusion coefficients of amorphous $SiO_2$ we rely on the expected value of the relative self-diffusion coefficient $D$(O)/$D$(Si). This ratio should ideally be 1.75, which is the ratio between the atomic weight of silicon and that of oxygen. In this case we see that the BKS [2] potential is relatively the best potential in reproducing the self-diffusion coefficients of amorphous $SiO_2$ at 1000 K. From Table 3 it can be seen that the BKS [2] potential is also relatively the best in reproducing the heat capacity at constant pressure of amorphous $SiO_2$. Regarding the isothermal compressibility of amorphous $SiO_2$ it is clear from Table 3 that the value predicted by the TTAM [1] potential is the closest to the experimental result, and that the BKS [2] potential is the second best potential in reproducing the isothermal compressibility of amorphous $SiO_2$. From the self-diffusion coefficients, heat capacity at constant pressure, and isothermal compressibility predicted in Table 3 we may conclude that the superiority of the BKS potential was further verified.

## 4. Conclusions

In summary, we assessed the quality of a series of well-known interatomic pair potentials frequently used in classical molecular dynamics simulations of amorphous $SiO_2$ based systems. We have tested the capabilities of these potentials in reproducing both the static structure of crystalline $SiO_2$, and both static structure and dynamical properties of amorphous $SiO_2$. It is concluded that quality of a given interatomic potential should be judged on the basis of which kind of properties are requested from a given classical molecular dynamics simulation. An interatomic potential performing very well in reproducing static structure of an amorphous system should not be naively selected to simulate other properties of this system. The current study confirms that only the potential developed by van Beest, Kramer, and van Santen (BKS) is able to adequately reproduce both static structure and dynamical properties of amorphous $SiO_2$.

We are grateful for funding from the UK Engineering and Physical Sciences Research Council (EPSRC). NA would like to thank Prof. A. Takada for very useful discussions and also Dr. C. Meneghini for providing Synchrotron X-ray diffraction data on amorphous $SiO_2$.

## References

[1] Tsuneyuki, S., Tsukada, M., Aoki, H., and Matsui, Y. *Phys. Rev. Lett.* **61**, 869 (1988).
[2] Beest, B. V., Kramer, G., and Santen, R. V., *Phys. Rev. Lett.* **64**, 1955 (1990).
[3] Cormack, A., Du, J., and Zeitler, T. *Phys. Chem. Chem. Phys.* **4**, 3193 (2002).
[4] Flikkema, E., and Bromley, S. *Chem. Phys. Lett.* **378**, 622 (2003).
[5] Du, J., and Cormack, A. *J. Non-Cryst. Solids* **351**, 2263 (2005).
[6] Pedone, A., Malavasi, G., Menziani, M., Cormack, A., and Segre, U. *J. Phys. Chem. B* **110**, 11780 (2006).
[7] Gale, J., and Rohl, A. *Mol. Simul.* **29**, 291 (2003).
[8] Smith, W., and Forester, T. *J. Mol. Graphics* **14**, 136 (1996).
[9] Afify, N. D., and Mountjoy, G. *Phys. Rev. B* **79**, 024202 (2009).
[10] Keen, D. A. *J. Appl. Cryst.* **34**, 172 (2001).
[11] Rg, T., Murzyn, K., Hinsen, K., and Kneller, G. *J. Comput. Chem.* **24**, 657 (2003).
[12] Taraskin, S., and Elliott, S. *Physica B* **234**, 452 (1997).
[13] Taraskin, S., and Elliott, S. *Phys. Rev. B* **55**, 117 (1997).
[14] Spearing, D. R., Farnan, I., and Stebbins, J. F. *Phys. Chem. Miner.* **19**, 307 (1992).
[15] Atansoff, J. V., and Hart, P. J. *Phys. Rev.* **59**, 85 (1941).
[16] Lawso, A. W. *Phys. Rev.* **59**, 838 (1941).
[17] Grimley, D., Wright, A., and Sinclair, R. *J. Non-Cryst. Solids* **119**, 49 (1990).
[18] Haworth, R., Mountjoy, G., Corno, M., Ugliengo, P., and Newport, R. *Phys. Rev. B* **81**, 060301 (2010).
[19] Sarnthein, J., Pasquarello, A., and Car, R. *Science* **275**, 1925 (1997).
[20] Saito, K., Kakiuchida, H., and Ikushima, A.J. *J. Appl. Phys.* **84**, 3107 (1998).
[21] *Handbook Optical Constants, ed Palik, V1, ISBN 0-12-544420-6*
[22] Rajabpour, A., Akizi, F.Y., Heyhat, M.M., and Gordiz, K. *Int. Nano. Lett.* **3**, 1 (2013).
[23] Ju, Y., Zhang, Q., Gong, Z. and Ji, G. *Chin. Phys. B* **22**, 083101 (2013).
[24] Kuzuu, N., Nagai, K., Tanaka, M., and Tamai, Y. *Jpn. J. Appl. Phys.* **44**, 8086 (2005).
[25] Le Roux, S., and Petkov, V. *J. Appl. Cryst.* **43**, 181 (2010).